Valence-Band Energy Dispersion in Modulation-Doped Quantum Wells: Effect of Strain and Confinement on Heavy- and Light-Hole Mixing

S. K. Lyo and E. D. Jones

Sandia National Laboratories, Albuquerque, New Mexico 87185

ABSTRACT. We present theory and data for the valence-band structure for lattice-matched, strained, symmetrically- and asymmetrically-doped quantum wells (QW's). Our self-consistent k•p calculation using a plane-wave basis (PWB) yields accurate results and can be applied to arbitrary potential profiles. The PWB is convenient for shallow as well as type II QW's (with the light-hole QW inverted due to strain). Excellent agreement is obtained between the theoretical dispersion curves and the data.

1. INTRODUCTION

A large hole mobility is desirable in many device applications. As is well known, one way to enhance the mobility is to reduce the mass as well as collisions with the impurities at low temperatures. Recently light in-plane mass was achieved in layered structures by introducing biaxial strain in the quantum well (QW) through crystal growth [1]. For example, in a strained $In_xGa_{1-x}As/GaAs$ QW, the light-hole (LH) band ($|3/2,\pm1/2\rangle$) is shifted down away from the valence-band edge while the heavy-hole (HH) band ($|3/2,\pm3/2\rangle$) is shifted up due to the compression in the QW. As a result, only the HH's with light in-plane mass are populated in typical modulation-doped QW's. Another way of achieving this kind of HH-LH separation is through a confinement effect. Namely, when the holes are confined in a QW, LH quantum levels move down relative to the HH levels in the valence band. A lattice-matched $GaAs/Al_xGa_{1-x}As$ QW is expected to show only the confinement effect with negligible strain effect. Therefore it is interesting to see the effect of the interplay between the strain and the confinement.

Recently valence-band structures of modulation-doped strained semiconductor single-quantum-wells (SQW's) such as $In_xGa_{1-x}As/GaAs$ were determined from magneto-luminescence [2]. The data indicate the importance of strain in determining the degree of HH-LH mixing and the hole masses for the motion in the QW plane [2]. The magneto-luminescence data from lattice-matched $GaAs/Al_xGa_{1-x}As$ QW's to be presented below clearly indicate the HH-LH separation through a confinement effect. The purpose of this paper is to present theory for the valence-band energy dispersion for lattice-matched and strained QW's and compare with the data. We consider symmetrically-doped and asymmetrically-doped SQW's and study how the strain and confinement affect the valence-band mass.

The low-energy valence-band structure is calculated by using a self-consistent k•p calculation. This method which can be applied to arbitrarily-shaped potential profiles is based on a plane-wave basis and yields numerically accurate results. The plane-wave basis is especially convenient for studying narrow or shallow QW's with only a few confined

levels as well as partially type II QW's (without any confined level) where the LH QW is inverted relative to the HH QW due to strain-induced shift of the LH-band bottom. For example, the LH band changes from type I to type II around $x \approx 0.2$ for $In_xGa_{1-x}As/GaAs$. The effect of the above mentioned LH QW inversion on the HH-LH mixing is studied for this system. Also, the conduction as well as valence bands are severely distorted by the fields from the dopant ions and the majority carries. The plane-wave basis is convenient for studying the effects of band bending on the valence-band structure. Excellent agreement is obtained between the theoretical valence-band energy dispersion curves and the data for both lattice-matched and strained QW's.

2. SELF-CONSISTENT K•P CALCULATION OF VALENCE-BAND ENERGY

The valence-band energy dispersion curve is calculated by diagonalizing the 4×4 block-diagonal Hamiltonian obtained from the Luttinger Hamiltonian through a unitary transformation [3] in the absence of an external magnetic field:

$$\begin{bmatrix} H^U & 0 \\ 0 & H^L \end{bmatrix} = \begin{bmatrix} F_+ & |I|+i|H| & 0 & 0 \\ |I|-i|H| & F_- & 0 & 0 \\ 0 & 0 & F_- & |I|+i|H| \\ 0 & 0 & |I|-i|H| & F_+ \end{bmatrix} \begin{matrix} |u_1\rangle \\ |u_2\rangle \\ |u_3\rangle \\ |u_4\rangle \end{matrix} \qquad (1)$$

where the orthogonal HH (LH) basis functions u_1 and u_4 (u_2 and u_3) are linear combinations $|3/2,\pm 3/2\rangle$ ($|3/2,\pm 1/2\rangle$) and

$$F_\pm = E_{v\pm}(z) + \frac{1}{2}(-\gamma_1 \pm 2\gamma_2)k_z^2 - \frac{1}{2}(\gamma_1 \pm \gamma_2)k^2, \qquad (2)$$

$$H = \sqrt{3}\gamma_3 k_- k_z \ , \quad I = \frac{\sqrt{3}}{2}(-\bar{\gamma}k_-^2 + \mu k_+^2). \qquad (3)$$

In (2) $E_{v\pm}(z)$ are the valence-band edges for HH's (+) and LH's (-), $k^2 = k_x^2 + k_y^2$, $k_z = \frac{\partial}{i\partial z}$ and $\hbar = m_o = 1$. Here m_o is the free electron mass. In (3) $k_\pm = k_x \pm ik_y$, $\bar{\gamma} = (\gamma_2 + \gamma_3)/2$, $\mu = (\gamma_2 - \gamma_3)/2$. In a lattice-matched SQW, the valence-band edges for the HH and LH are degenerate (i.e., $E_{v+} = E_{v-}$) as shown in Fig. 1a. In a strained SQW such as $In_xGa_{1-x}As/GaAs$ with the growth direction (i.e., the z-axis) in the [100] direction, for example, the effect of the compression inside the QW is to raise $E_{v+}(z)$ and lower $E_{v-}(z)$ inside the QW by Δ_+ (> 0) and Δ_- (> 0), respectively, as shown in Fig. 1b. Therefore the well is deeper for the HH than for the LH. The LH QW may even become inverted under a large strain as indicated by a dashed line in the figure.

When the band-edge potentials have an inversion symmetry (i.e., $E_{v\pm}(-z) = E_{v\pm}(z)$), the 2×2 Hamiltonians H^U and H^L are equivalent, so that the HH and LH band edges are degenerate [3]. The degeneracies are lifted in the absence of the inversion symmetry. In order to diagonalize H^U (or H^L) we introduce a sinusoidal-wave basis set:

$$\psi_{en} = (2/d)^{1/2}\cos k_n z, \qquad k_n = (2n-1)\pi/d$$
$$\psi_{on} = (2/d)^{1/2}\sin k_n z, \qquad k_n = 2n\pi/d \tag{4}$$

for the HH as well as LH states where $n = 1, 2, \cdots, n_{max}$ and $z = 0$ is the center of the QW. The wave functions in (4) are assumed to vanish for $|z| > d/2$. The quantity d is arbitrary but is chosen to be much larger than the QW width b in order to avoid the cut-off effect. Also, the final result is independent of n_{max} for large n_{max}. When the γ-parameters depend on z, the kinetic-energy terms in (2) are rewritten in a Hermitian form [4]: $k_z(-\gamma_1 \pm \gamma_2)k_z/2$. This expression insures the continuity of the current. Also, the quantity H in (3) is replaced by $H = (\sqrt{3}k_-/2)(\gamma_3 k_z + k_z\gamma_3)$.

If we ignore the interactions of the hole with the dopant ions and the majority carriers, the valence-band energy-dispersion curve is obtained by diagonalizing H^U (or H^L). For typical QW structures considered here with $b < 120$ Å, a very rapid convergence is obtained for $d = 1000$ Å and $n_{max} = 150$. However, the QW is severely distorted by Coulomb fields arising from the electrons (for n-type samples considered in this paper) and dopant ions, complicating the problem. For an n-type system we find the potential profile of the conduction band first. For this purpose we evaluate the matrix elements of the Hamiltonian $H_c = k_z\gamma_c k_z/2 + E_c(z)$ for the conduction band in terms of the basis set given in (4). Here γ_c is the inverse mass of the conduction electron in the growth direction and $E_c(z)$ is the square-well potential of depth V_c. The electron distribution is found from the eigenfunctions of H_c at 0 K and the Coulomb potential from the electrons and ions is calculated. We add these Coulomb potential to the original H_c and diagonalize the new H_c and recalculate the new Coulomb potential. Iterating this procedure, we find that the charge distribution and the potential profile converge very fast to self-consistent values usually after three iterations. This process yields at the same time the Coulomb-potential profile for the holes, which is added to $E_{v\pm}(z)$ in (2). The valence-band energy dispersion is then obtained by diagonalizing H^U (H^L).

3. NUMERICAL RESULTS AND COMPARISON WITH DATA

The γ-parameters used for applications are $\gamma_1 = 6.85$, $\gamma_2 = 2.1$, $\gamma_3 = 2.9$ for GaAs and $\gamma_1 = 20.4$, $\gamma_2 = 8.3$, $\gamma_3 = 9.1$ for InAs [5]. The compositional-average γ-values are used for $In_xGa_{1-x}As/GaAs$ QW. The samples to be studied below are of n-type. However, the magneto-luminescence technique can measure the energy-dispersion curves for both the conduction and valence bands [2]. We first study a 45 Å-wide $GaAs/Al_{0.25}Ga_{0.75}As$ SQW with an electron density $N = 6.6\times10^{11}$ cm^{-2}. Only one side of the QW is doped with Si following a 70 Å-wide undoped $Al_{0.25}Ga_{0.75}As$ buffer layer. The ions are calculated to be uniformly spread out within a 51 Å-wide layer at 0 K. A more detailed description of the sample is given in Ref. [6]. The conduction and valence band offsets equal approximately 284 meV and $V_o = 135$ meV (see Fig. 1), respectively. The theoretical energy-dispersion curve for the HH agrees well with the data as shown in Fig. 2. The LH energies are separated away from the HH energies through confinement effect and are not shown there. It is seen that the HH and LH mixing alters the energy dispersion significantly. The degree of HH-LH mixing depends on the QW width, which determines the HH and LH separations and their wave functions.

We now consider a symmetric 80 Å-wide Si-doped $GaAs/In_{0.2}Ga_{0.8}As/GaAs$ QW with $N = 5\times10^{11}$ cm^{-2} [2]. The width of the undoped GaAs buffer layers on both sides of the QW equals 100 Å. The ions are distributed over 17 Å-wide layers at 0 K. The conduction and HH band offsets equal approximately 128 meV and $V_{HH} = 67$ meV (cf. Fig. 1), respectively. The LH band is assumed to lie approximately $\Delta = \Delta_+ + \Delta_- = 57$ meV below the HH band and is a shallow QW (of type I) of depth $V_{LH} = 10$ meV (cf. Fig. 1). The theoretical energy dispersion curve is compared with the data [2] in Fig. 3. Again the agreement is excellent. The amount of HH-LH mixing and therefore the mass are much smaller here than in Fig. 2, because the HH-LH separation in $In_{0.2}Ga_{0.8}As/GaAs$ is mainly strain-induced and, as a result, is much larger than that in $GaAs/Al_{0.25}Ga_{0.75}As$, which arises from the confinement effect alone. Because there are uncertainties in Δ, we increased Δ to $\Delta = 67$ meV and $\Delta = 77$ meV corresponding to a flat LH band (i.e., $V_{LH} = 0$) and an inverted (i.e., type II) LH band (indicated by a dashed line in Fig. 1), respectively, in order to see if there is any significant change in the fitting. No significant change was found except that the HH-LH mixing diminished somewhat and the curves were shifted up slightly relative to that of $\Delta = 57$ meV in Fig. 3 for large wave numbers.

The theoretical energy dispersion curves in Figs. 2 and 3 are obtained by fully taking into account the band bending. We calculated the dispersion curves ignoring Coulomb fields, namely for simple square-well potentials. Apart from a uniform shift of a few meV of the HH ground level, nearly the same dispersion curves were obtained for both cases, indicating that band-bending effects are not important. This is consistent with the fact that only a slight shift to the electron charge distribution was found even when an asymmetric band-bending (as for the above lattice-matched case) is introduced. Namely, the electrons are rigidly locked in the QW unless the

QW is very wide (> 500 Å). We find negligible spin-splitting for the asymmetrically doped QW.

In summary we presented theory and data for the valence-band structure for lattice-matched, strained, symmetrically- and asymmetrically-doped QW's. Our self-consistent k.p calculation using a plane-wave basis yielded excellent agreement with the data for both the strained and unstrained systems. The major difference between the strained and unstrained systems is simply the size of the HH-LH separations in the strained system.

The authors acknowledge valuable conversations with I. J. Fritz, G. C. Osbourn, and C. P. Tigges. This work was supported by the U.S. DOE under Contract No.DE-AC04-76DP00789

References

1. G. C. Osbourn, P. L. Gourley, I. J. Fritz, R. M. Biefeld, L. R. Dawson, and T. E. Zipperian, in Semiconductors and Semimetals, Vol. 24, 459, Eds. R. K. Willardson and A. C. Beer, Academic Press (New York, 1987).
2. E. D. Jones, S. K. Lyo, I. J. Fritz, J. F. Klem, J. E. Schirber, C. P. Tigges, and T. J. Drummond, Appl. Phys. Lett. 54, 2227 (1989).
3. D. A. Broido and Sham, Phys. Rev. B 31, 888 (1985).
4. R. A. Morrow and K. R. Brownstein, Phys. Rev. B 30, 678 (1984).
5. Landolt-Bónstein Series, Vol. 22, 82-120, Ed. O. Madelung, Springer (New York, 1987).
6. E. D. Jones, S. K. Lyo, J. F. Klem, J. E. Schirber, and.K.Lin, Proceedings: Gallium Arsenide and Related Compound-1991.

Figure Captions

Fig. 1 Heavy-hole and light-hole valence-band edges for (a) lattice-matched and (b) strained quantum wells.

Fig. 2 Comparison of theoretical in-plane energy dispersion along [100] of heavy hole with the data from 45 Å-wide GaAs/$Al_{0.25}Ga_{0.75}As$. The warping is found to be small.

Fig. 3 Comparison of theoretical in-plane energy dispersion along [100] of heavy hole with the data from 80 Å-wide $In_{0.2}Ga_{0.8}/GaAs$. The warping is found to be negligible.

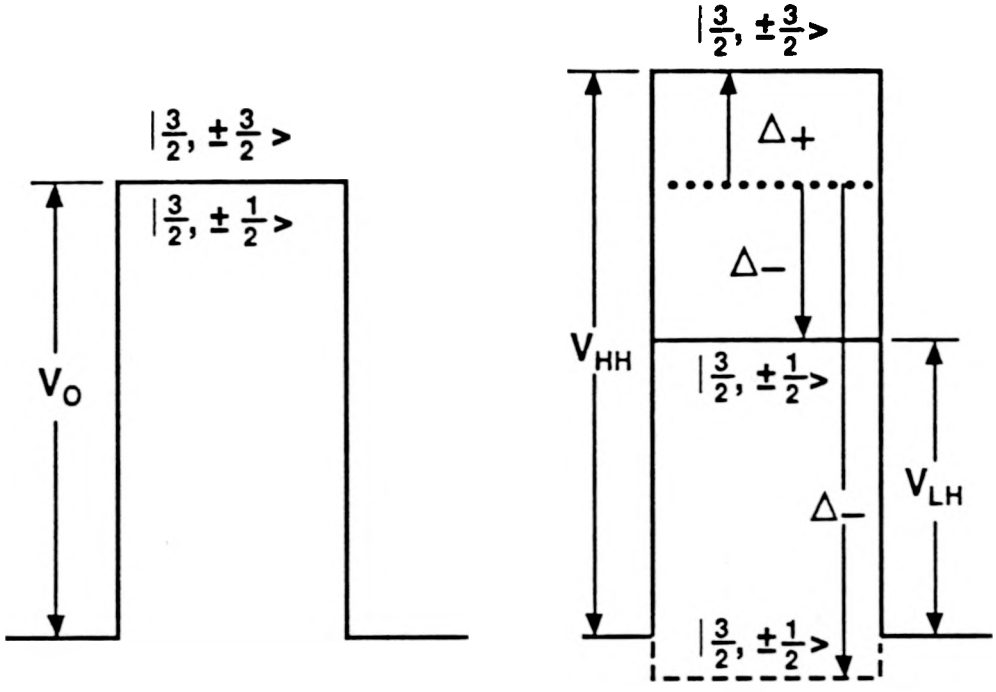
$|\frac{3}{2}, \pm\frac{3}{2}>$
$|\frac{3}{2}, \pm\frac{1}{2}>$
V_O
$|\frac{3}{2}, \pm\frac{3}{2}>$
Δ_+
Δ_-
V_{HH}
$|\frac{3}{2}, \pm\frac{1}{2}>$
Δ_-
V_{LH}
$|\frac{3}{2}, \pm\frac{1}{2}>$
Unstrained
(a)
Strained
(b)

FIG. 1

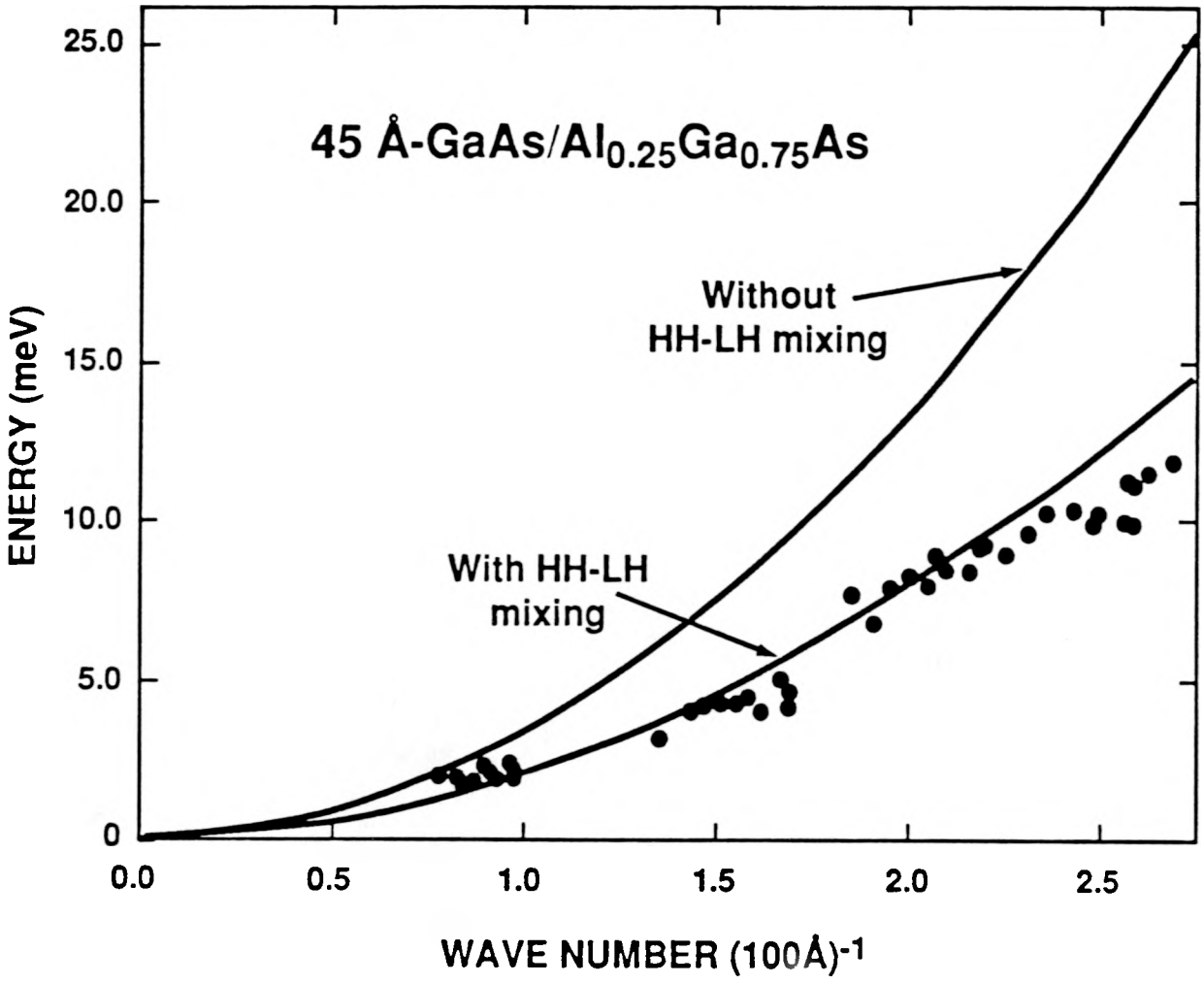
45 Å-GaAs/Al0.25Ga0.75As
Without
HH-LH mixing
With HH-LH
mixing
ENERGY (meV)
25.0
20.0
15.0
10.0
5.0
0
0.0
0.5
1.0
1.5
2.0
2.5
WAVE NUMBER (100Å)-1

FIG. 2

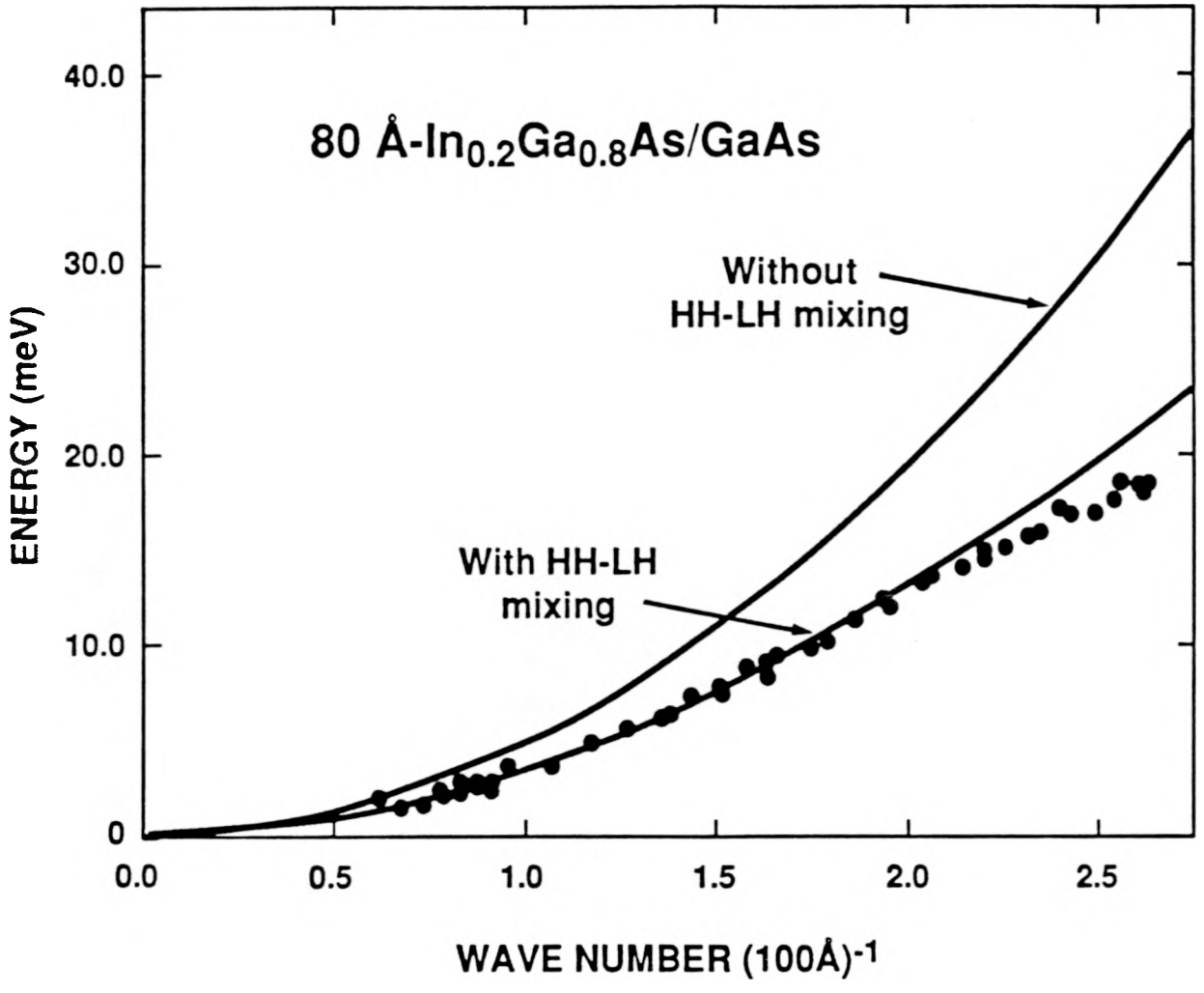
80 Å-In0.2Ga0.8As/GaAs
Without
HH-LH mixing
With HH-LH
mixing
ENERGY (meV)
40.0
30.0
20.0
10.0
0
0.0
0.5
1.0
1.5
2.0
2.5
WAVE NUMBER (100Å)-1

FIG. 3